Coordinated control of Notch-Delta signalling and cell cycle progression drives lateral inhibition mediated tissue patterning

Ginger L. Hunter[1,7], Zena Hadjivasiliou[2,3], Hope Bonin[1], Li He[4], Norbert Perrimon[4], Guillaume Charras[5, 6,7], and Buzz Baum[1,7]

[1]MRC-Laboratory for Molecular and Cell Biology, University College London, London, WC1E 6BT, UK

[2]Centre for Mathematics, Physics, and Engineering in the Life Sciences and Experimental Biology, University College London, London, WC1E 6BT, UK

[3]Department of Genetics, Evolution and Environment, University College London, London, WC1E 6BT, UK

[4]Howard Hughes Medical Institute, Department of Genetics, Harvard Medical School, Boston, MA, 02115, USA

[5]London Centre for Nanotechnology, University College London, London, WC1E 6BT, UK

[6]Department of Cell and Developmental Biology, University College London, WC1E 6BT, UK

[7]Institute of Physics of Living Systems, University College London, WC1E 6BT, UK

Corresponding Author: g.hunter@ucl.ac.uk

Senior Corresponding Author: b.baum@ucl.ac.uk

Keywords: Notch signalling, cell cycle, lateral inhibition, patterning, G2-phase

Summary Statement

During tissue refinement in the fly notum, signal-induced cellular decision-making is coordinated with cell division in both space and time to ensure that cell fate decisions are properly patterned.

Abstract

Coordinating cell differentiation with cell growth and division is critical for the successful development, homeostasis, and regeneration of multicellular tissues. Here we use bristle patterning in the fly notum as a model system to explore the regulatory and functional coupling of cell cycle progression and cell fate decision-making. The pattern of bristles and intervening epithelial cells (ECs) becomes established through Notch-mediated lateral inhibition during G2-phase of the cell cycle, as neighbouring cells physically interact with each other via lateral contacts and/or basal protrusions. Since Notch signalling controls cell division timing downstream of Cdc25, ECs in lateral contact with a Delta-expressing cell experience higher levels of Notch signalling and divide first, followed by more distant neighbours, and lastly Delta-expressing cells. Conversely, mitotic entry and cell division makes ECs refractory to lateral inhibition signalling, fixing their fate. Using a combination of experiments and computational modeling, we show that this reciprocal relationship between Notch signalling and cell cycle progression acts like a developmental clock, providing a delimited window of time during which cells decide their fate, ensuring efficient and orderly bristle patterning.

Introduction

In the Drosophila notum, Notch-mediated lateral inhibition drives the emergence of a patterned array of microchaete, or small mechanosensory bristles, ~8-18 hours after pupariation (AP) at 25°C (Fig 1A, Movie S1) (Simpson et al., 1999; Furman and Bukharina, 2008; Cohen et al., 2010). Cells with low levels of activated Notch signalling adopt a sensory organ precursor cell (SOP) fate, and divide to give rise to the microchaete lineage (Simpson, 1990). Moreover, SOPs express high levels of neural precursor genes and Delta ligand (Muskavitch, 1994; Parks et al., 1997), which activates Notch signalling in surrounding cells to prevent them from adopting a neural fate (Muskavitch, 1994). In this way, Notch-Delta signalling breaks symmetry to pattern the tissue (Parks et al., 1997). Notch signalling in this tissue is not limited to lateral cell contacts: a network of dynamic, actin-based protrusions at the basal side of the epithelium aids signal propagation over longer distances (De Joussineau et al., 2003; Cohen et al., 2010). This type of protrusion-mediated signalling (Hamada et al., 2014; Kornberg and Roy, 2014; Khait et al., 2016), it has been argued (Cohen et al., 2010; Cohen et al., 2011), helps ensure the gradual emergence and refinement of a pattern of well-spaced SOPs.

Work across eukaryotic systems suggests that the decision to exit the cell cycle and divide often occurs in G1 (Vidwans and Su, 2001; Lee and Orr-Weaver, 2003). Nevertheless, some cell fate decisions, including the development of macrochaete (Usui and Kimura, 1992; Kimura et al., 1997; Negre et al., 2003), appear to be made during passage through G2. In this paper, we show how feedback between cell fate determining signals and progression through mitosis coordinates timely epithelial patterning in the fly notum.

Results and Discussion

During notum development, all ECs divide once (Bosveld et al., 2012)(Movie S1), before undergoing terminal differentiation. At the same time, an initially disordered array of cells expressing proneural genes is refined to generate an ordered pattern of bristles in adults (Cohen et al., 2010; Protonotarios et al., 2014)(Fig 1A). By simultaneously following cell division and patterning in this tissue, we find that local patterns of division timing correlate with proximity to SOPs (Fig 1B-D). ECs sharing long cell-cell interfaces with SOPs, hereafter termed *primary-neighbours*, divide first. These are followed by next-nearest ECs, or *secondary-neighbours*, which likely contact SOPs via dynamic basal protrusions alone (Cohen et al., 2010). SOPs divide last (Fig 1C). The local spatiotemporal pattern of divisions is robust, as indicated by a ratio of division times for neighbours surrounding each SOP of <1 (Fig. 1E), even though the timing of bristle rows patterning is developmentally staggered (Usui and Kimura, 1993; Parks et al., 1997). Moreover, ECs that transiently express proneural markers (Cohen et al., 2010)(Fig S1A-C), including Delta (Kunisch et al., 1994), before assuming an EC fate accelerate G2-exit in their EC neighbours (Fig 1F).

The local pattern of EC division is Notch-dependent

If lateral inhibition cues division timing, as suggested by these observations, we can make the following predictions. First, for each SOP neighbourhood, there should be differences in the intensity of Notch signalling between primary and secondary neighbours. Second, perturbing Notch signalling should disrupt the pattern of cell divisions. To test this, we visualized signalling

dynamics using *Notch-nls:sfGFP* (N^{sfGFP})(Fig 2A-B). N^{sfGFP} is a nuclear localized, PEST-tagged (unstable), super-folder GFP expressed downstream of a minimal GBE-Su(H) promoter (He and Perrimon, unpublished)(Li et al., 1998; Furriols and Bray, 2001)(Fig S1A-C).

At 12h AP, N^{sfGFP} is visible in EC rows in which bristle formation occurs (Fig S1A)(Usui and Kimura, 1993). Notch signalling increases nearly linearly in ECs until division (Fig 2C; S1D-G). The rate of response, which functions as a measure of signal strength, is higher in primary than secondary neighbours (Fig 2C-D). The peak N^{sfGFP} signal is similar for both neighbours when measured across the tissue (Fig 2E). However, the local ratio of N^{sfGFP} signal prior to division is >1 (Fig 2F), suggesting that primary ECs receive a higher Delta signal from individual SOPs than secondary ECs.

To test whether N^{sfGFP} signal and division timing in ECs depends on Delta expression in SOPs, we measured local N^{sfGFP} signal following laser ablation of SOPs (Fig S1H). Under these conditions, N^{sfGFP} signal accumulation halts in primary and secondary ECs, but continues to increase in ECs proximal to both the wound *and* intact SOPs (Fig S1I), as expected if the signal depends on a Delta input from the ablated SOP. Relative to controls, EC divisions are delayed following local SOP loss (Fig S1J). Additionally, we found that dominant negative Delta ligand ($Delta^{DN}$) overexpression in SOPs decreases N^{sfGFP} signal in neighbouring ECs (Fig 2G-H)(Herranz et al., 2006). Together with the ablation data, this shows that N^{sfGFP} signal in ECs is dependent upon Delta-expressing SOPs.

Next we examined the effects of disrupting Notch signalling on cell division timing by overexpressing $Delta^{DN}$ in SOPs (Fig 2I) or using RNAi against

Suppressor of Hairless (Su(H)), an essential component of Notch-targeted gene expression (Lehman et al., 1999; Furriols and Bray, 2001) across the tissue. Delta^{DN} expression did not disrupt the pattern of local division timings but was sufficient to delay division of neighbouring ECs, as expected if Delta signal promotes division. Su(H) depletion blocks divisions within the *pnr* domain in the majority of animals (N = 4/6 pupae), and later leads to tissue failure. In the remaining animals (N = 2/6 pupae), which may express levels of Su(H) activity sufficient for tissue survival, divisions are delayed and the local pattern of divisions is perturbed in regions where microchaete are formed (Fig 2J). Therefore, local cell division timing is dependent on Notch-mediated lateral inhibition.

The local timing of EC division is cdc25/wee1 dependent.

At the onset of bristle patterning, cells in the notum are arrested in G2 of the cell cycle. All cells express a nuclear FUCCI-GFP marker (Fig S2A) without staining for EdU, a marker for ongoing DNA replication (Fig S2B). In many systems, G2-exit is regulated by Cdc25 phosphatase, encoded by Drosophila *string (stg)* (Edgar and O'Farrell, 1989; Courtot et al., 1992), which catalyses removal of an inhibitory phosphate group (added by Wee1/Myt1 kinases (Price et al., 2000; Jin et al., 2008)) from a regulatory tyrosine on Cdk1. The kinases Wee1/Myt1 function in opposition to Cdc25 in many systems (Vidwans and Su, 2001), sometimes redundantly (Jin et al., 2008).

To test whether Cdc25 and Wee1/Myt1 regulate G2-exit in the notum, we expressed dsRNAs targeting these regulators under pnr-GAL4. *cdc25RNAi* expression delays EC division timing, prevents patterned divisions, and in some

cases blocks division altogether (Fig 3A-A'; S2C). Conversely, *wee1*- or *myt1RNAi* expression throughout the notum causes precocious EC entry into mitosis (Fig 3B-C). Loss of *cdc25* or *wee1/myt1* expression does not affect the timing of the first division of SOPs (Fig 3A-C)(which are subject to additional regulation (Ayeni et al., 2016)). Together, these results support a model in which the opposing activities of Cdc25 and Wee1/Myt1 regulate EC division timing.

Conversely, the duration of G2 may influence Notch signalling. Since N^{sfGFP} decreases immediately after EC divisions, but *prior* to SOP division (Fig 3D-E), we investigated whether division renders ECs refractory to Delta signal. To test this, we quantified N^{sfGFP} dynamics in cells in which the length of G2 was altered by *cdc25*- or *wee1RNAi*. As expected if division curtails signalling, N^{sfGFP} expression was retained in cells with extended G2 (Fig 3D-F), but was lost in those that divided prematurely (Fig 3D-E). The timing of G2-exit appears to be critical for a robust Notch response in ECs, which is terminated following division.

Relative timing of SOP cell and EC division is critical for bristle patterning.

To examine the consequences of observed coupling between Notch signalling and cell cycle progression on tissue patterning we developed a mathematical model of lateral inhibition (see Supplemental Methods for details)(Cohen et al., 2010; Sprinzak et al., 2010). The model follows the dynamics of transmembrane Notch receptor (*N*), Delta ligand (*D*), and intracellular Notch (*R*; *i.e.,* activated Notch) in a 2D-array of cells. We model basal protrusion mediated signalling (relevant for 1N, 2N) and signalling mediated by apicolateral cell-cell contacts (relevant for 1N only). The level of apical and basal

signalling is weighted by α_a and α_b, respectively; we set $\alpha_a > \alpha_b$ following previous observations (Benhra et al., 2010; Cohen et al., 2010). To couple signalling and division, we allow cells to divide with a probability p_d at any time step, as a function of R, so that:

$$p_d = \frac{R^q}{K_R^q + R^q}$$

The value of K_R determines the window of Notch response for which division becomes likely (Fig S3A). To mimic events in the tissue, after division the developmental fate of a cell is locked and it no longer participates in lateral inhibition.

To model a wildtype tissue where Notch signalling drives EC division, we set q=5 and K_R=200 (Fig 4A; S3B-D). Under these conditions, primary neighbours divide first, followed by secondary neighbours (Fig 4B-C), consistent with spatiotemporal patterning of EC division *in vivo* (Fig 1C-E); a delay that persists even when $\alpha_a=\alpha_b$ (*i.e.,* amount of apical or basal Delta is equivalent; Fig. S3E). The overall profile of Notch expression at division in neighbours generated by the model (Fig S3D) is comparable to that seen *in vivo* (Fig S1D-G). At the tissue level, the time taken to reach a stable pattern increases with K_R (Fig S3F), suggesting that for a given developmental time window, there is an optimal range of Notch response for determining cell fate.

Using this model, we tested the effect of uncoupling EC division timing from Notch signalling: any (non-Delta) cell may divide with a fixed probability p_d, that is independent of Notch. This leads to sparse patterns with few Delta cells, particularly for large values of p_d (Fig 4D; S3G). We also tested the effect of primary and secondary neighbours dividing at the same time (Fig S3H) by only

allowing uniform protrusion-based signalling – where signal strength is independent of protrusion length. Under these conditions the pattern is again ordered but sparse. Together, this suggests that the delay in division in cells with low Notch expression is important for patterning. Because patterning is not uniform across the notum, this delay (Fig 1C and 4B-C) preserves a pool of ECs that, because they lie far from SOPs and receive a weak Delta-input signal (Fig 2D-F), have the potential to switch fate to help refine the bristle pattern as it emerges (Movie S1).

Next we investigated the impact of changing the relative timing of SOP and EC divisions. When we couple Delta expression to a fixed value of p_d, so that cells whose Delta expression exceeds a threshold (D_{th}) can divide, clusters of Delta expressing cells form that disrupt the pattern (Fig 4E). This is because, under the model, a Delta cell that divides no longer inhibits its neighbours from acquiring an SOP fate. To test whether we observe similar behavior *in vivo*, we overexpressed Cdc25/String in SOPs (Fig 4F-I). This disrupts tissue patterning in two ways. First, we observe cells expressing low levels of *neuralized* reporter dividing early. Frequently, one daughter cell develops into an SOP, and the other is inhibited from doing so, switching to EC cell fate (47.5%, n=61; N=3) or delaminating (9.8%). In other cases both daughter cells form SOPs (26.2%, Fig 4H) and paired bristles (Fig S3I). Second, we observed secondary neighbours of early dividing SOPs adopting an SOP fate (Fig 4I), as in the model, likely following the loss of protrusion-mediated Delta signalling at division. We note that this phenotype is also observed on occasion in wildtype tissue, and is consistent with the observation that precocious SOP division terminates Delta signalling, leading to reduced levels of N^{sfGFP} signal in surrounding ECs (Fig S3J-

K). These data further support our hypothesis that cell division signals the termination of lateral inhibition between SOPs and ECs.

Conclusions

The results of our experimental analysis show that Notch signalling drives EC division in the notum, coupling patterning to cell cycle progression. As shown in simulations, this aids timely and orderly patterning by taking cells "out of the game", so that the fate of ECs is sealed before SOPs divide. The effects of rewiring the system can be seen by the induction of premature SOP divisions, which in both experiment and model leads to the formation of excess SOPs as the result of secondary ECs changing their fate. The delay in the division of secondary and tertiary ECs, which receive a relatively weaker Delta input from local SOPs, provides a population of cells with an indeterminate fate that can be used to fill in any gaps in the pattern as it emerges. This is key to pattern refinement. Through an extended G2, the system has a delimited window of time during which Notch-Delta can pattern the tissue through lateral inhibition, before signal induced entry into mitosis fixes the pattern, driving the process to completion.

Materials and Methods.

Fly strains. 'Wildtype' refers to control animals. See Supplemental Information for full list.

Microscopy. White pre-pupae were picked and aged to 12h AP at 18°C. Live pupae dissected as previously described (Zitserman and Roegiers, 2011). Live-pupae were imaged on Leica SPE confocal, 40x oil immersion objective (1.15NA) at room temperature. Fixed nota were imaged on Leica SPE3 confocal, 63x oil immersion objective (1.3NA). Datasets captured using Leica LSM AF software.

Laser Ablation. Ablations performed with 730-nm multiphoton excitation from a Chameleon-XR Ti–Sapphire laser on a Zeiss Axioskop2/LSM510 (AIM, Zeiss). Post-ablation images acquired as described above.

Immunofluorescence. Nota of staged pupae fixed as previously described (Zitserman and Roegiers, 2011)(Supplemental Information). Primary antibodies: anti-GFP (1:1000, AbCam); anti-Dlg (1:500, DSHB). Secondary antibodies: AlexaFluor anti-chicken 488, anti-mouse 568 (both 1:1000). EdU staining was performed using Clik-it EdU imaging kit (ThermoFisher).

Quantitation. N^{sfGFP} signal quantified as follows: unprocessed imaging data was imported into FIJI (ImageJ, NIH). Mean pixel value for a nuclear ROI was taken for each time point. Normalized N^{sfGFP} is relative to N^{sfGFP} signal at t_0. For neighbourhood measurements, nuclear ROIs were taken and averaged for 4-5 primary and 4-5 secondary ECs per SOP in bristle row 2. Internal control measurements were made in the same animals, but outside the pnr domain. For cell division timing panels, T = 0 min at ~12h AP. Resulting data was analyzed using Prism (Graphpad) and using statistical tests as outlined in figure legends.

Mathematical model. See Supplemental Information.

Author Contributions G.H., Z.H., and B.B. wrote the manuscript. G.H. and B.B. designed experiments. G.H. performed and analyzed fly experiments, aided by H.B. Z.H. designed and implemented 2D modeling. L.H. and N.P. designed, generated, and provided N^{sfGFP} fly lines. G.C. and B.B. acquired funding.

Acknowledgements. Laser ablation experiments were performed with the help of Jonathan Gale (UCL). We thank Jonathan Clarke (KCL) for critical reading of this manuscript. Stocks obtained from the Bloomington Drosophila Stock Center (NIH P40OD018537) were used in this study. Work in the Perrimon lab was supported by NIH (R21) and HHMI. Z.H. was supported by an EPSRC Research Fellowship (EP/L504889/1). G.H. was supported by BBSRC (BB/J008532/1). B.B. was supported by CRUK fellowship and UCL. The authors declare no financial conflict of interest.

References

Ayeni, J. O., Audibert, A. s., Fichelson, P., Srayko, M., Gho, M. and Campbell, S. D. (2016) 'G2-phase arrest prevents bristle progenitor self-renewal and synchronizes cell divisions with cell fate differentiation', *Development (Cambridge, England)*.

Benhra, N., Vignaux, F. o., Dussert, A., Schweisguth, F. o. and Le Borgne, R. (2010) 'Neuralized promotes basal to apical transcytosis of delta in epithelial cells', *Molecular biology of the cell* 21(12): 2078-2086.

Bosveld, F., Bonnet, I., Guirao, B., Tlili, S., Wang, Z., Petitalot, A., Marchand, R. l., Bardet, P.-L. L., Marcq, P., Graner, F. o. et al. (2012) 'Mechanical control of morphogenesis by Fat/Dachsous/Four-jointed planar cell polarity pathway', *Science (New York, N.Y.)* 336(6082): 724-727.

Cohen, M., Baum, B. and Miodownik, M. (2011) 'The importance of structured noise in the generation of self-organizing tissue patterns through contact-mediated cell-cell signalling', *Journal of the Royal Society, Interface / the Royal Society* 8(59): 787-798.

Cohen, M., Georgiou, M., Stevenson, N. L., Miodownik, M. and Baum, B. (2010) 'Dynamic filopodia transmit intermittent Delta-Notch signaling to drive pattern refinement during lateral inhibition', *Developmental cell* 19(1): 78-89.

Courtot, C., Fankhauser, C., Simanis, V. and Lehner, C. F. (1992) 'The Drosophila cdc25 homolog twine is required for meiosis', *Development* 116(2): 405-16.

De Joussineau, C., Soul√¯©, J., Martin, M., Anguille, C., Montcourrier, P. and Alexandre, D. (2003) 'Delta-promoted filopodia mediate long-range lateral inhibition in Drosophila', *Nature* 426(6966): 555-559.

Edgar, B. A. and O'Farrell, P. H. (1989) 'Genetic control of cell division patterns in the Drosophila embryo', *Cell* 57(1): 177-87.

Furman, D. P. and Bukharina, T. A. (2008) 'How Drosophila melanogaster Forms its Mechanoreceptors', *Current genomics* 9(5): 312-323.

Furriols, M. and Bray, S. (2001) 'A model Notch response element detects Suppressor of Hairless-dependent molecular switch', *Current biology : CB* 11(1): 60-64.

Hamada, H., Watanabe, M., Lau, H. E., Nishida, T., Hasegawa, T., Parichy, D. M. and Kondo, S. (2014) 'Involvement of Delta/Notch signaling in zebrafish adult pigment stripe patterning', *Development (Cambridge, England)* 141(2): 318-324.

Herranz, H., Stamataki, E., Feiguin, F. and Milan, M. (2006) 'Self-refinement of Notch activity through the transmembrane protein Crumbs: modulation of gamma-secretase activity', *EMBO reports* 7(3): 297-302.

Jin, Z., Homola, E., Tiong, S. and Campbell, S. D. (2008) 'Drosophila myt1 is the major cdk1 inhibitory kinase for wing imaginal disc development', *Genetics* 180(4): 2123-2133.

Khait, I., Orsher, Y., Golan, O., Binshtok, U., Gordon-Bar, N., Amir-Zilberstein, L. and Sprinzak, D. (2016) 'Quantitative Analysis of Delta-like 1 Membrane Dynamics Elucidates the Role of Contact Geometry on Notch Signaling', *Cell reports* 14(2): 225-233.

Kimura, K., Usui-Ishihara, A. and Usui, K. (1997) 'G2 arrest of cell cycle ensures a determination process of sensory mother cell formation in Drosophila', *Development Genes and Evolution*.

Kornberg, T. B. and Roy, S. (2014) 'Cytonemes as specialized signaling filopodia', *Development (Cambridge, England)* 141(4): 729-736.
Kunisch, M., Haenlin, M. and Campos-Ortega, J. A. (1994) 'Lateral inhibition mediated by the Drosophila neurogenic gene delta is enhanced by proneural proteins', *Proceedings of the National Academy of Sciences of the United States of America* 91(21): 10139-43.
Lee, L. A. and Orr-Weaver, T. L. (2003) 'Regulation of cell cycles in Drosophila development: intrinsic and extrinsic cues', *Annual review of genetics* 37: 545-578.
Lehman, D. A., Patterson, B., Johnston, L. A., Balzer, T., Britton, J. S., Saint, R. and Edgar, B. A. (1999) 'Cis-regulatory elements of the mitotic regulator, string/Cdc25', *Development (Cambridge, England)* 126(9): 1793-1803.
Li, X., Zhao, X., Fang, Y., Jiang, X., Duong, T., Fan, C., Huang, C. C. and Kain, S. R. (1998) 'Generation of destabilized green fluorescent protein as a transcription reporter', *The Journal of biological chemistry* 273(52): 34970-5.
Muskavitch, M. A. (1994) 'Delta-notch signaling and Drosophila cell fate choice', *Developmental biology* 166(2): 415-430.
Negre, N., Ghysen, A. and Martinez, A. M. (2003) 'Mitotic G2-arrest is required for neural cell fate determination in Drosophila', *Mechanisms of development* 120(2): 253-65.
Parks, A. L., Huppert, S. S. and Muskavitch, M. A. (1997) 'The dynamics of neurogenic signalling underlying bristle development in Drosophila melanogaster', *Mechanisms of Development* 63(1): 61-74.
Price, D., Rabinovitch, S., O'Farrell, P. H. and Campbell, S. D. (2000) 'Drosophila wee1 has an essential role in the nuclear divisions of early embryogenesis', *Genetics* 155(1): 159-66.
Protonotarios, E. D., Baum, B., Johnston, A., Hunter, G. L. and Griffin, L. D. (2014) 'An absolute interval scale of order for point patterns', *Journal of the Royal Society, Interface / the Royal Society* 11(99).
Simpson, P. (1990) 'Lateral inhibition and the development of the sensory bristles of the adult peripheral nervous system of Drosophila', *Development (Cambridge, England)* 109(3): 509-519.
Simpson, P., Woehl, R. and Usui, K. (1999) 'The development and evolution of bristle patterns in Diptera', *Development* 126(7): 1349-64.
Sprinzak, D., Lakhanpal, A., Lebon, L., Santat, L. A., Fontes, M. E., Anderson, G. A., Garcia-Ojalvo, J. and Elowitz, M. B. (2010) 'Cis-interactions between Notch and Delta generate mutually exclusive signalling states', *Nature* 465(7294): 86-90.
Usui, K. and Kimura, K. (1992) 'Sensory mother cells are selected from among mitotically quiescent cluster of cells in the wing disc of Drosophila', *Development* 116: 601-610.
Usui, K. and Kimura, K.-i. (1993) 'Sequential emergence of the evenly spaced microchaetes on the notum of Drosophila', *Roux's archives of developmental biology* 203(3): 151-158.
Vidwans, S. J. and Su, T. T. (2001) 'Cycling through development in Drosophila and other metazoa', *Nature cell biology* 3(1): E35-9.
Zitserman, D. and Roegiers, F. (2011) 'Live-cell imaging of sensory organ precursor cells in intact Drosophila pupae', *Journal of visualized experiments : JoVE*(51).

Figures

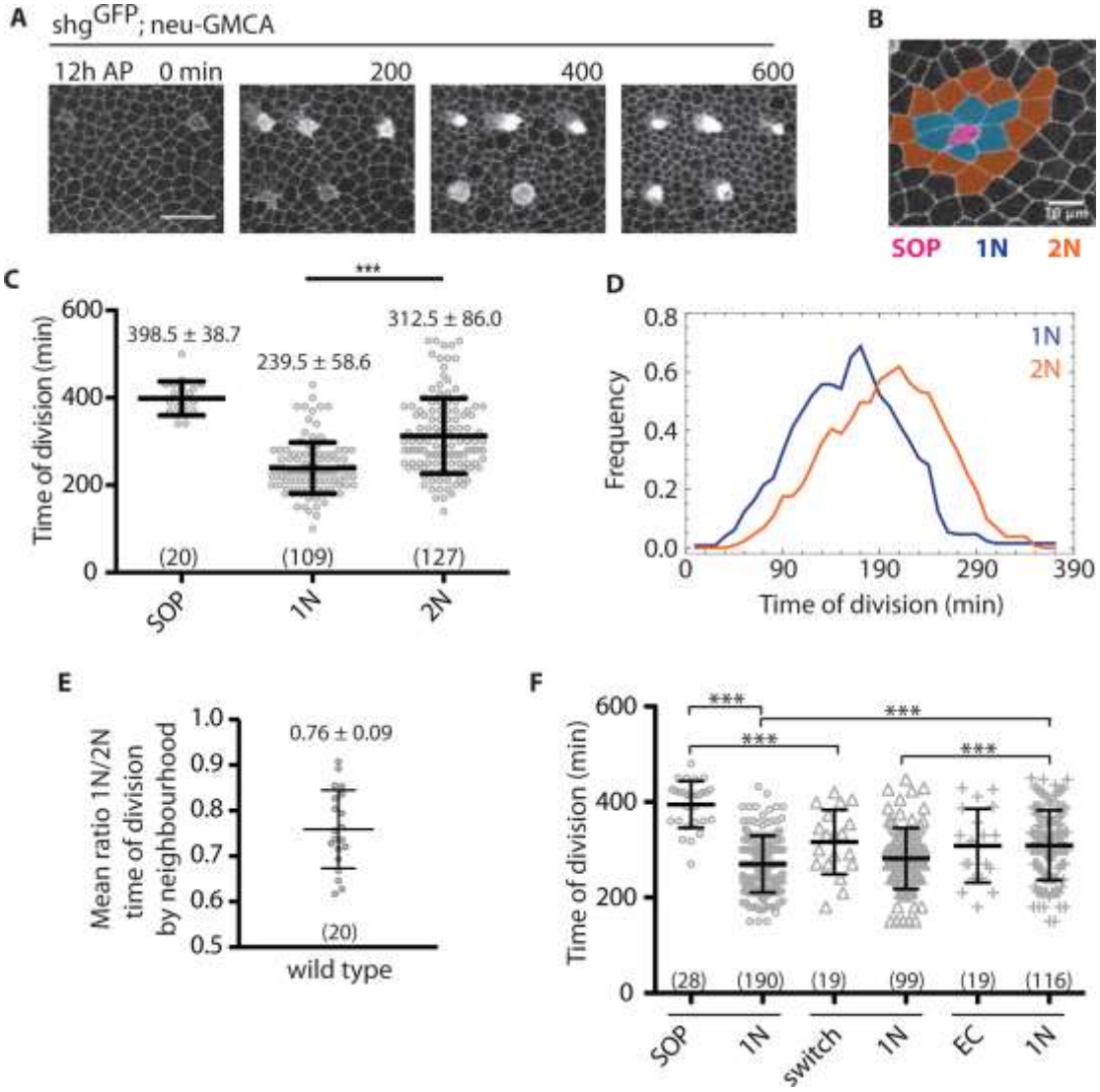

Figure 1. Spatiotemporal patterning of notum cell divisions. (A) Pupal notum expressing shotgun^{GFP} (cell boundaries), and nGMCA (SOPs) over time. All nota: posterior-left, anterior-right. Scale bar, 25 μm. (B) SOP 'neighbourhood': SOP (pink), primary (1N, blue), and secondary neighbours (2N, orange). Scale bar, 10 μm. (C) Time of cell division in genotype (A); (n)=number of cells, N=2 pupae.

(D) Histogram of data in (C). (E) Mean ratio of local SOP neighbourhood division timing, genotype as in (A). N=2 nota; n=20 SOPs, 109 1Ns, 127 2Ns. (F) Division timing of SOPs, Switch (neu-GMCA expressing cells that switch to EC fate) and ECs and their 1Ns in shotgun^{GFP}; neu-GMCA pupae (N=3). ***, p<0.001 unpaired, two-tailed, t-test for pairs indicated. Mean±SD shown.

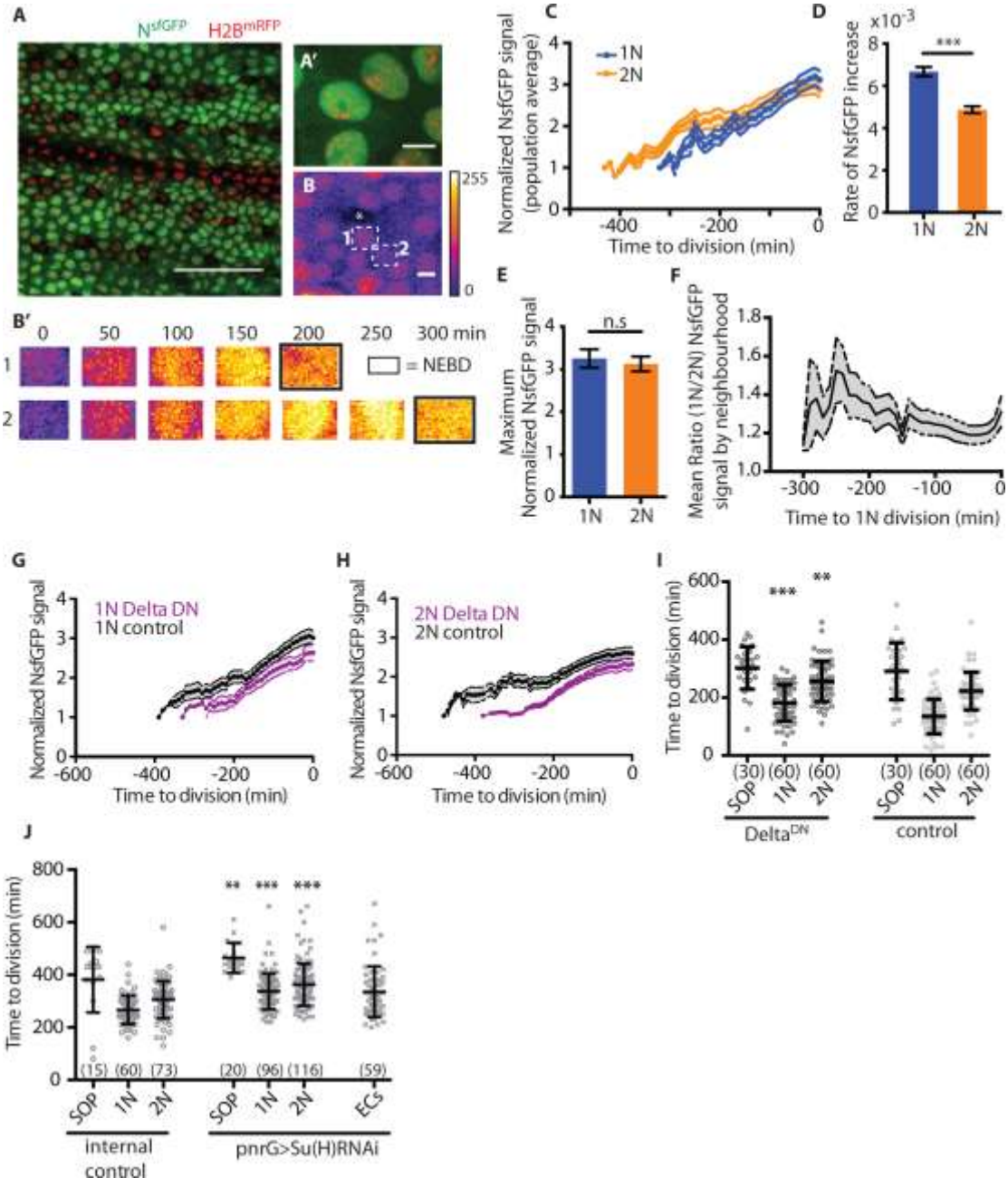

Figure 2. Cell division timing depends on Notch signalling. N^{sfGFP} expression pattern (A) at 12h AP, $H2B^{mRFP}$ labels nuclei. Scale bar, 50 μm. (A') Higher magnification image of (A), scale bar, 5μm. (B) False colored panel of N^{sfGFP} expressing ECs. Asterisk=SOP. Primary (1) and secondary (2) neighbour. Scale

bar, 5μm. (B') Time series of nuclear ROIs for cells 1 and 2 until nuclear envelope breakdown (NEBD), leading to transient depletion of signal. (C) N^{sfGFP} dynamics in ECs (n=29 each, N=3). (D) Rate of N^{sfGFP} increase for data in (C). (E) Maximum normalized N^{sfGFP} signal for data in (C). (F) Mean ratio of local SOP neighbourhood N^{sfGFP} signal (n=27 SOP, 133 each EC type; N=3). (G-I) neur-GAL4 expression of $Delta^{DN}$ reduces Notch signalling in wildtype (G) 1N or (H) 2N cells (n=16, N=2) vs. control (UAS-lifeActRuby, n=30, N=3) and (I) delays cell division timing in $shotgun^{GFP}$; neu-GAL4, UAS-GMCA>UAS-$Delta^{DN}$ pupae (N=3). (K) Cell division timing in $shotgun^{GFP}$; pnrGAL4>UAS-Su(H) RNAi pupae relative to control (N=2). ECs = epithelial cells in regions lacking differentiating SOPs. Mean±SEM for (C,F,G,H); Mean±SD for (D,E,I,J). **, p <0.01; ***, p<0.0001 by unpaired, two-tailed t-test as indicated to control of same type (*i.e.,* RNAi-1N to control-1N).

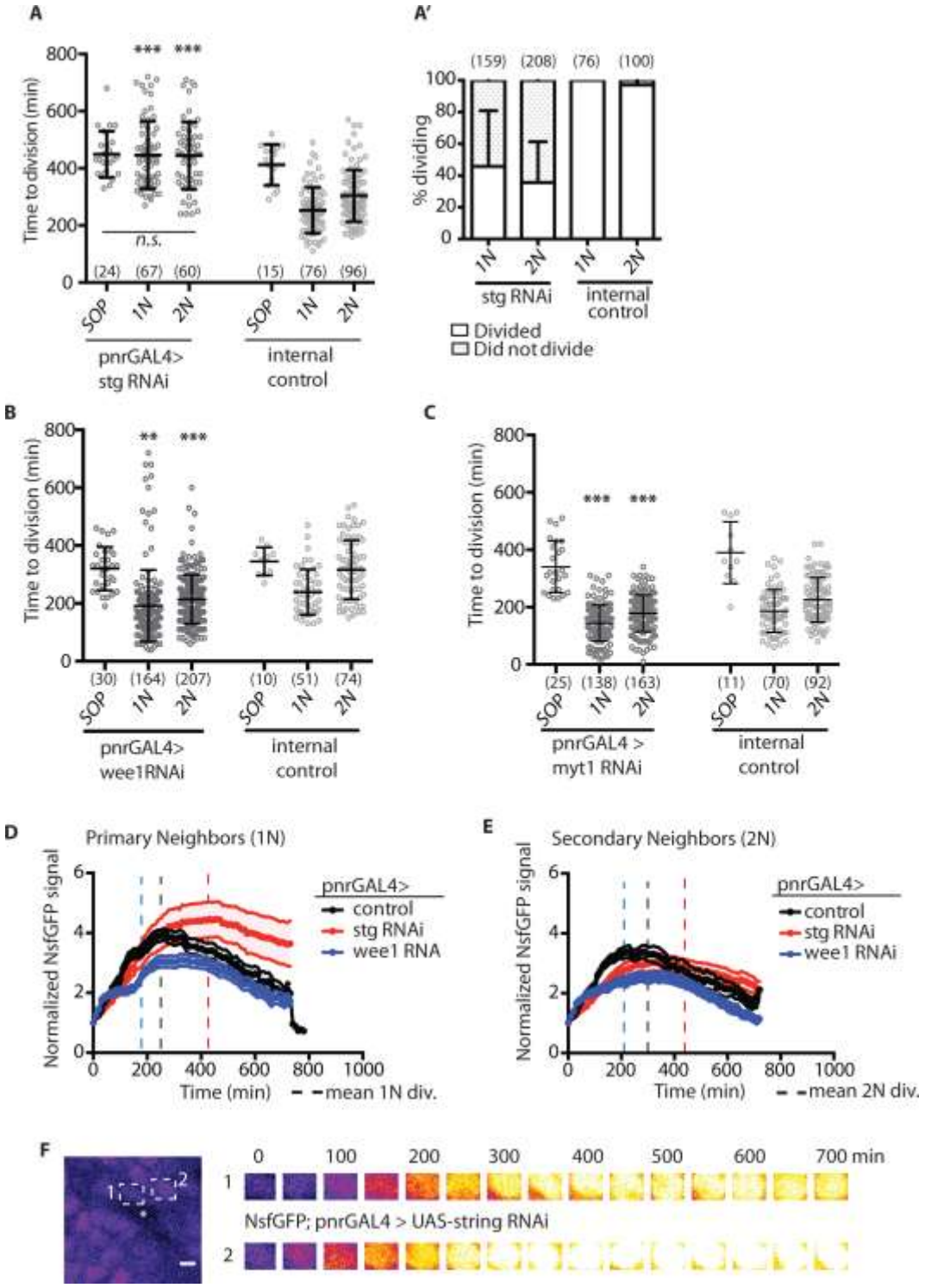

Figure 3. Regulation of notum division timing. (A) Cell division timing in shotgun^{GFP}; pnrGAL4>UAS-stringRNAi pupae (N=3). n.s., not significant by one-

way ANOVA. (A') Percent dividing cells in genotype as (A). Cell division timing in shotgun^{GFP}; pnrGAL4> (B) UAS-wee1RNAi(N=3) or (C) UAS-myt1RNAi pupae (N=3). For all panels, mean±SD shown, (n) = number of cells. (D,E) N^{sfGFP} dynamics (mean±SEM) in (D) primary and (E) secondary neighbour ECs expressing UAS-stgRNAi (red, n=20, N=2), UAS-wee1RNAi (blue, n=20, N=2), or control (UAS-lifeActRuby, black, n=30, N=3) under pnr-GAL4. Vertical dashed lines indicate mean cell division timing for cell position and genotype. (F) Time series of nuclear ROIs for *stringRNAi* expressing cells 1 and 2, showing failure to downregulate signal. NEBD does not occur. **, p≤0.01; ***, p≤0.001 by unpaired, two-tailed, t-test to control of same type.

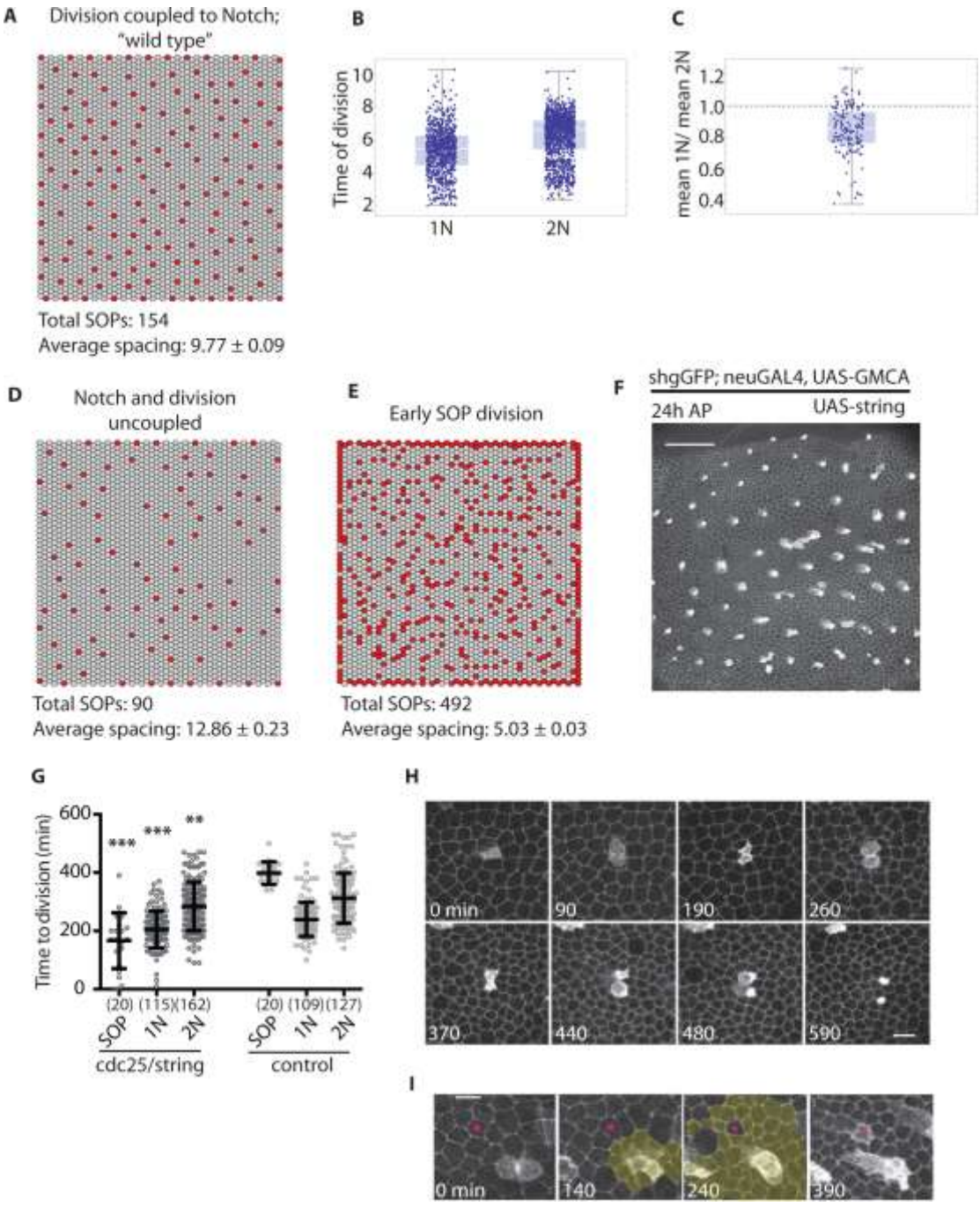

Figure 4. Cell division timing is critical for SOP patterning. (A) Model output for 'wildtype' simulation (K_R=200, q=5). Average spacing is the mean ±SEM distance between each SOP and its 10 nearest SOPs. (B) Simulation results for cell

division timing in 1N and 2N, wildtype model as in (A). (C) Ratio of mean time of division for 1N and 2N in the model. (D) Model output when Notch signalling and division timing are uncoupled, p_d=0.005 (any non-Delta cell [D < 1] divides with probability p_d). (E) Model output when SOPs are forced to divide early (Delta cells [D>1] divide with probability p_d=0.0001). Red = Delta expressing SOPs (D>1); uncolored = Notch expressing ECs. (F) Final SOP pattern in tissues with precocious SOP division. Scale bar, 50μm. (G) Cell division timing in shotgun^{GFP}; neu-GAL4, UAS-GMCA>UAS-string pupae (N=3, mean±SD). Control = shotgun^{GFP}; neu-GAL4, UAS-GMCA (N=3). (H) SOP 'twins' and (I) secondary neighbour cell switching (asterisk), as a consequence of precocious SOP division as in (F). Yellow=divided cells. Scale bars, 10μm. ** p≤0.01, *** p≤0.001, unpaired, two-tailed, t-test to control of same type.

Supplemental Information

Movie S1, related to Figure 1. SOP pattern development. Notum genotype: shotgun:GFP, neun GAL4, UASn GMCA. Anterior to the right. Scale bar, 50µm. Timelapse (upper left, hh:mm), 1 frame = 30 minutes.

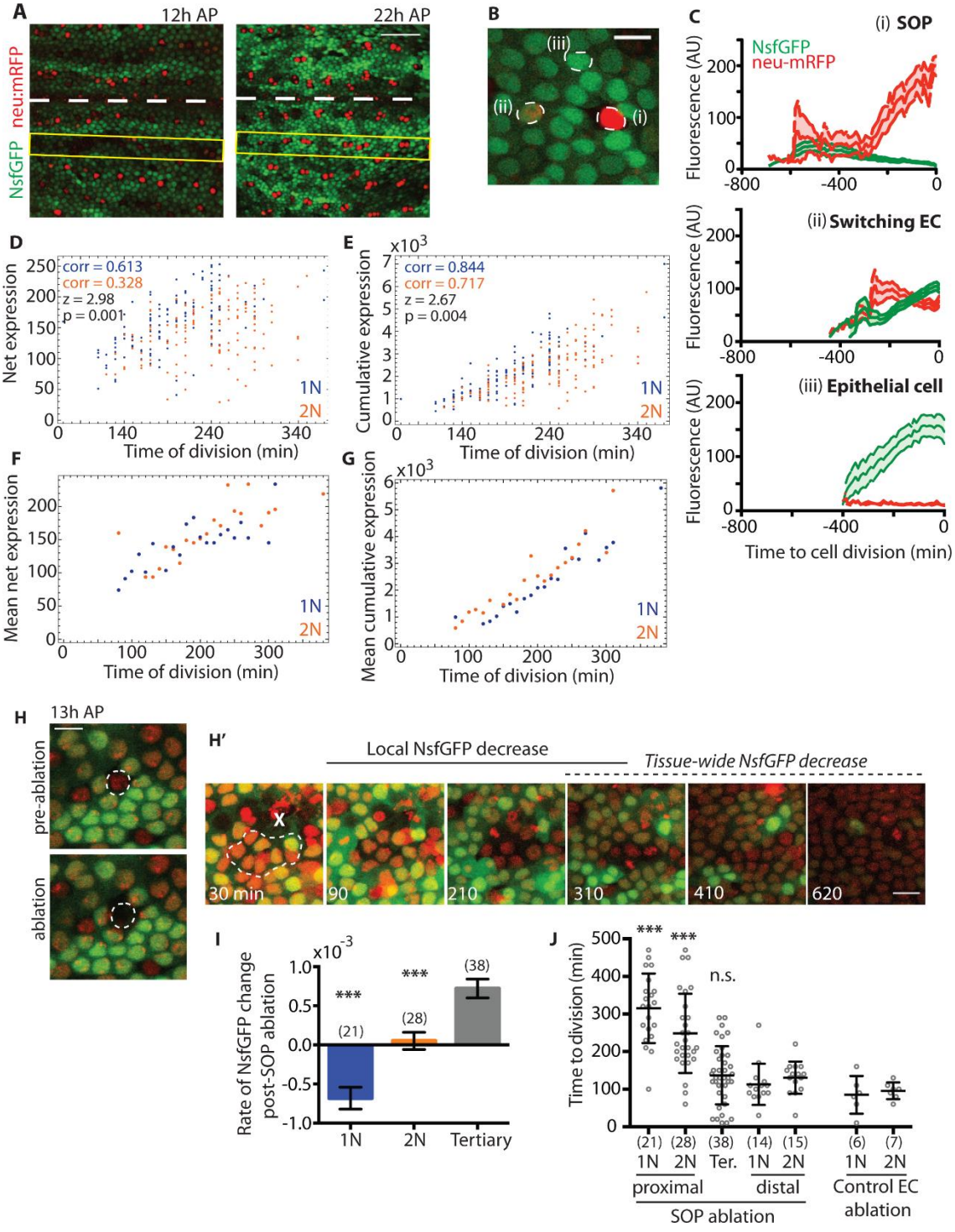

Figure S1, related to Figure 2. (A) Notum expressing N^{sfGFP} (green) indicating Notch response and neu-mRFP (red) indicating pro-neural gene expression at 12 and 22h AP. Dashed line indicates midline. Yellow box highlights bristle row 2. Unless otherwise indicated, N^{sfGFP} measurements were made for developing SOP neighbourhoods in row 2. Scale bar, 50μm. (B) N^{sfGFP} and neu-mRFP expressing notum cells, indicating cells expressing (i) only pro-neural reporter, (ii) both reporters, or (iii) only Notch reporter. Scale bar, 10μm. (C, i-iii) Corresponding N^{sfGFP} and neu-mRFP dynamics in (i) SOP cells (n = 7, N = 2), (ii) cells expressing both reporters (n = 35, N = 3), and (iii) epithelial cells (n = 6, N = 1). Mean ± SEM. (D, E) Plot of individual data points corresponding to net (D) or cumulative (E) NsfGFP expression. (F) Mean net N^{sfGFP} levels at the time of division increases with time of division. (G) Mean cumulative N^{sfGFP} expression increases with time of division. (D-G) n=266 cells, N=3 nota; corr = Pearson's correlation coefficient, z-value = Fisher r-to-z transformation, p-value = one-tailed test, 1N>2N.
(H) Notum expressing N^{sfGFP} (green) indicating Notch response and ubi-H2B-mRFP (red) indicating nuclei 13h AP. Pre-ablation and post-ablation panels, targeted SOP cell is outlined. In pre-ablation image, the indicated SOP is the only SOP in the panel. Scale bar, 10μm. (H') Example of post-ablation tissue (from region in H). White dashed line indicates cells that are primary and secondary neighbours to the ablated SOP cell (marked with X). Local NsfGFP decrease precedes tissue-wide NsfGFP decrease, suggesting that loss of SOP leads to acute loss of Notch response. Cell division occurs (*e.g.,* see panel at 310 min) and epithelium heals. (I) Rate of change of normalized NsfGFP fluorescence in ECs neighbouring an ablated SOP cell as in (H'). 1N, primary neighbour to ablated SOP; 2N, secondary neighbour to ablated SOP; tertiary, cells 2N+ to ablated SOP,

but ≤ 2N to an nearby, intact, SOP. Data generated from a total 5 ablations performed across 3 pupae, (n) = number of cells. Rate measured from onset of timelapse imaging, beginning 30 min after ablation, ~13.5h APF. *** $p \leq 0.001$, One-way ANOVA, multiple comparisons, comparing to tertiary cells. Mean ± S.D. shown. (J) Cell division is delayed following SOP ablation. 1N, proximal: primary neighbour to ablated SOP; 2N, proximal: secondary neighbour to ablated SOP; ter.: tertiary cells as defined in (I); 1N, distal: primary neighbours to an intact SOP in same notum as proximal cells, but >100 μm away (as a developmental timing control); 2N, distal: secondary neighbors to an intact SOP in the same notum as proximal cells, but >100 μm away; 1N, control EC ablation: primary neighbor to an ablated EC (SOPs intact, as a wounding control); 2N, control EC ablation: secondary neighbor to an ablated EC (SOPs intact). Two control EC ablations were performed in one pupae. (n) = number of cells. T = 0 at ~13.5hAP. Mean ± S.D. shown. *** $p \leq 0.001$, by One-way ANOVA, multiple comparisons, comparing to tertiary cells. N.s., by one-way ANOVA using control 1N groups.

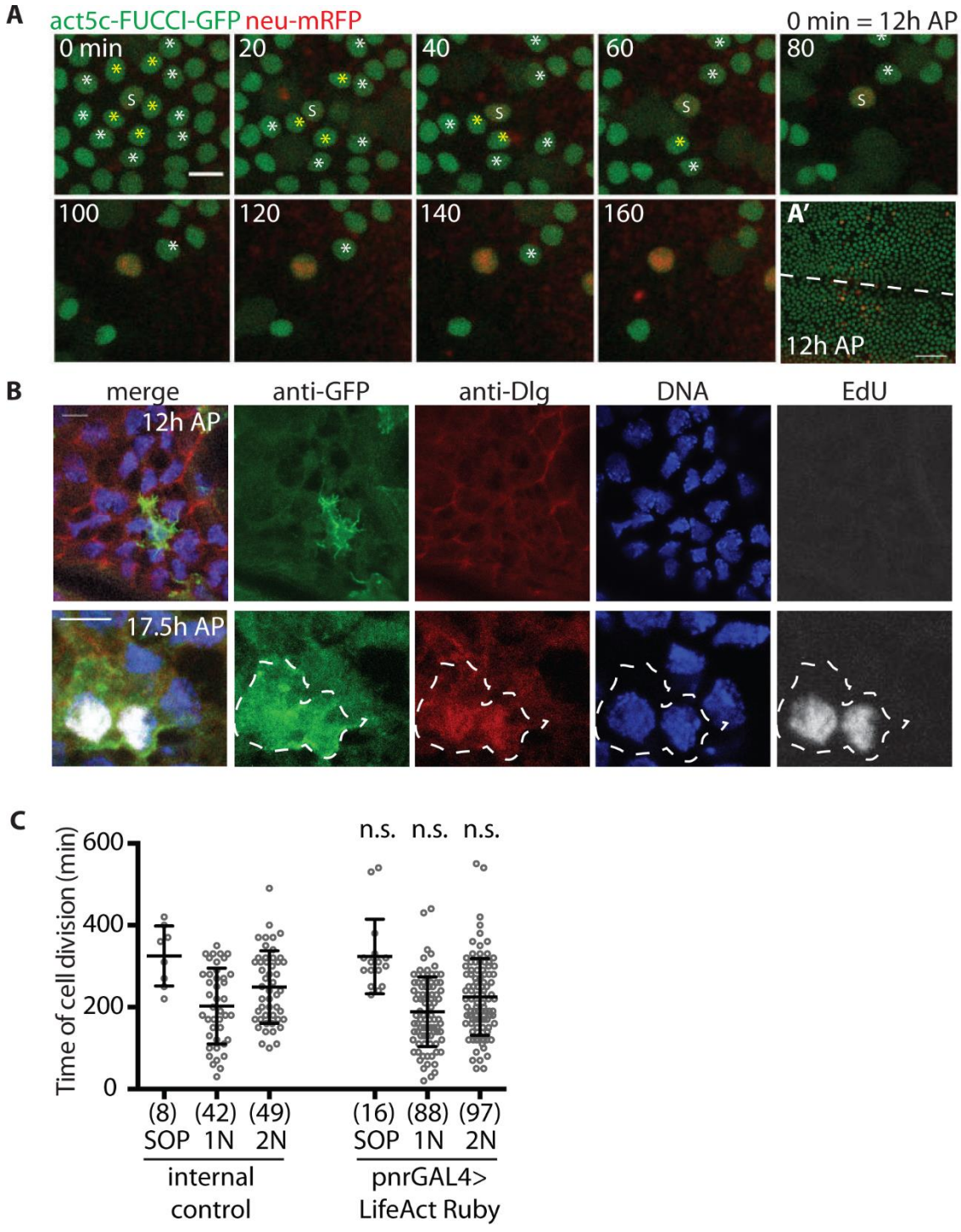

Figure S2, related to Figure 3. (A) act-FUCCI-GFP (green) and neu-mRFP (red). Loss of GFP signal indicates G2-exit. S, SOP cell; yellow asterisk, 1N; white asterisk, 2N. Scale bar, 10 μm. (A') Zoomed out image of full FUCCI-GFP expressing nota; scale bar, 50 μm, dashed line indicates midline. All cells are in G2. (B) 12h (upper panels) and 17.5h (lower panels) AP nota labeled with EdU to indicate absence of ECs in S-phase; cell cycle progression in SOP cell lineage serves as a control. Genotype: neu-GAL4, UAS-GMCA; thus anti-GFP panels visualize GMCA/F-actin in SOP or SOP daughter (pIIa/pIIb) cells. Dashed white line outlines pIIa/pIIb cell bodies. Scale bar, 5 μm. (C) Cell division timing in shotgun^{GFP}, neu-GMCA; pnrGAL4 > UAS-LifeActRuby control pupae (N=2, n = as noted). N.s., not significant by unpaired t-test, compared by cell type (i.e., 1N inside vs 1N outside). Cells counted outside pnr domain as internal control to inside pnr domain UAS expressing cells.

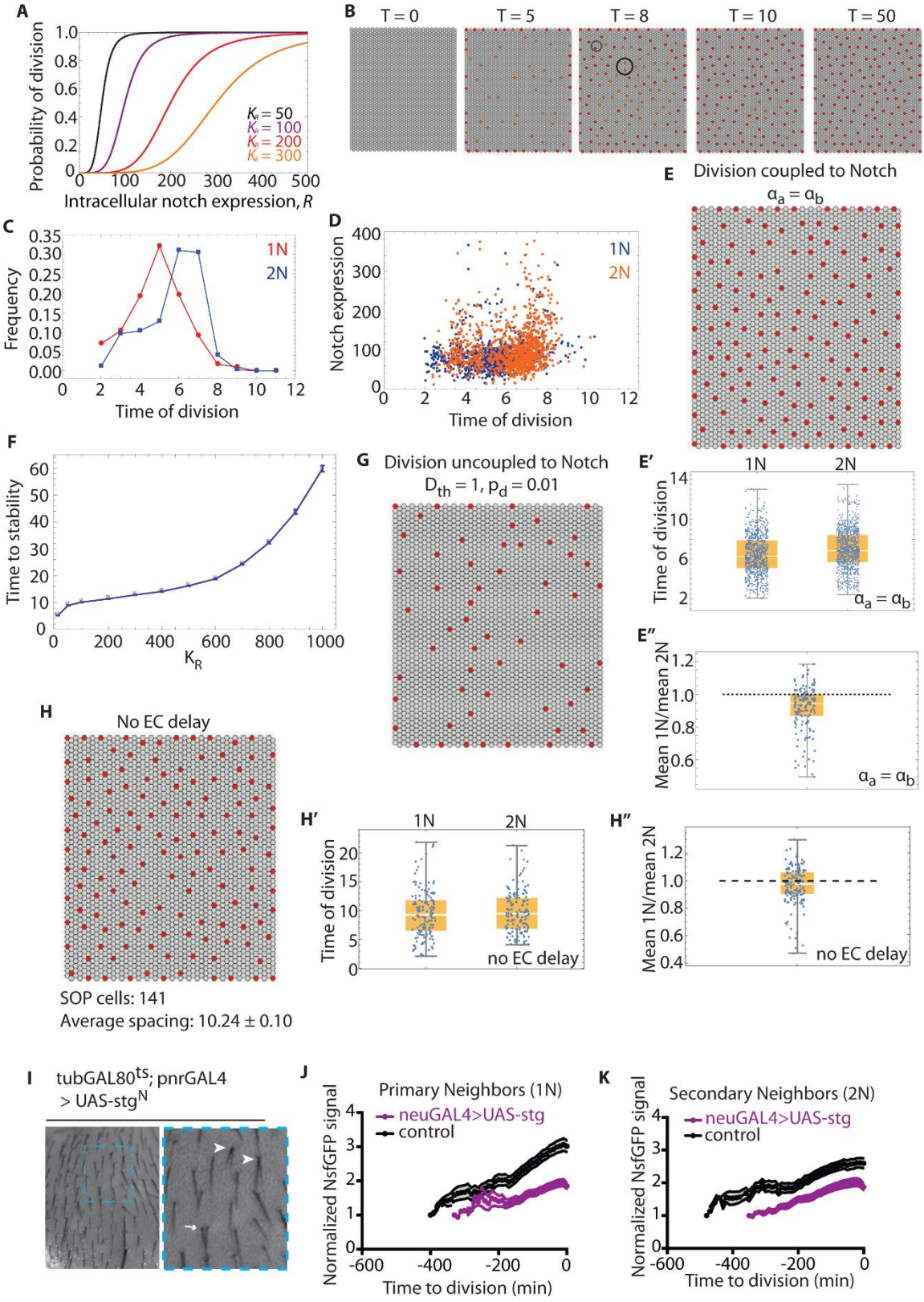

Figure S3, related to Figure 4. (A) Probability of division for given values of K_R and q=5. (B) Time course of 'wildtype' pattern, R_{th} = 200, p_d = 0.5. Red cells = high Delta; Orange cells = intermediate; Uncolored/gray = high Notch. Circles indicate local, transient pattern disruptions that are resolved. (C) Frequency of divisions for the wildtype model by time-step. (D) Level of Notch expression (AU) at division time for dividing cells in the wildtype model. (E) Model output when cell division is coupled to Notch but $\alpha_a = \alpha_b$. (E') Timing of 1N and 2N cell divisions when $\alpha_a = \alpha_b$. (E'') Local ratio of mean 1N and mean 2N time of divisions when $\alpha_a = \alpha_b$. (F) Time to stability for given values of R_{th}. Stability is defined as >2 AU of time without cell fate changes in the pattern. (G) Final time point for simulations where cell division is uncoupled from Notch signaling for D_{th} and p_d indicated. (H) Model output when cell division is coupled to Notch but independent of protrusion length, with $\alpha_a = 0$, $\alpha_b = 1.2$ (thus 1N and 2N ECs have equivalent incoming Notch signal; there is no delay between mean 1N and mean 2N division time) (H') Timing of 1N and 2N cell divisions and (H'') local ratio of mean 1N and mean 2N time of divisions for simulation as in (H). (I) Adult dorsal thorax microchaete patterns of the genotypes indicated. Anterior to the top of each panel. Arrowheads indicate split microchaete; arrow indicates 'twin' adjacent microchaete. (J) N^{sfGFP} signal dynamics in wild type primary or (K) secondary ECs neighbouring SOPs overexpressing cdc25/string (stg) under neu-GAL4 (purple; n=28, N= 3) or control SOPs (black; neuGAL4, UAS-lifeActRuby; n = 30, N=3). Mean ± SEM shown.

Supplemental Experimental Procedures

Fly strains. Drivers: tub-GAL80^{ts}/CyO; neuralized-GAL4, UAS-GMCA/TM6B

neu-GAL4, UAS-GMCA/TM6B

shotgun^{GFP}; neu-GAL4, UAS-GMCA/TM6B

shotgun^{GFP}, neu-GMCA/CyO-GFP; pnr-GAL4/TM6B

N^{sfGFP}/CyO-GFP; pnr-GAL4/TM6B

N^{sfGFP}/CyO-GFP; neu-GAL4/TM6B

Responders: UAS-wee1RNAi; UAS-myt1RNAi; UAS-stg RNAi; UAS-Su(H) RNAi; UAS-lifeActRuby; UAS-string^{N}.

Other: N^{sfGFP}; act-FUCCI-GFP; neuralized-nls:mRFP

Immunofluorescence. Nota were fixed in 4% formaldehyde / 1x PBS (Sigma) and washed to permeablize with 1x PBS with 0.01% Triton X-100 (1x PBST). Samples were blocked (50% blocking buffer: 3% FBS, 5% BSA in 1x PBS) for 1h at room temperature. Primary antibodies (anti-Discs-large, DSHB 4F3, Parnas et al., Neuron 2001; anti-GFP, AbCam, ab#13970) were added to 5% blocking buffer in 1x PBST to concentrations listed, and incubated overnight at 4°C. Samples were washed several times with 1x PBST, and incubated in secondary antibody in 1x PBST at room temperature for 2-4 h. Where needed, nota were further incubated for 20 min at room temperature with phalloidin (Acti-stain 555 phalloidin, Cytoskeleton PHDH1-A, 1:500) and DAPI (Molecular Probes D1306, 1:1000) or Hoechst33342 (provided with Clik-it EdU kit, ThermoFisher C10340, 1:2000). Final washes in 1x PBST were followed by overnight equilibration in mounting media (50% glycerol/1x PBS).

Mathematical Methods in Full

Protein dynamics

We used a mathematical model to simulate lateral inhibition by Delta-Notch signalling. The model is defined by a set of coupled differential equations (based on (S1)), which describe the dynamics of Notch (N_i), Delta (D_i) and a Reporter of Notch signalling (R_i) for individual cells:

$$\frac{dN_i}{dt} = \beta_N - \frac{N_i D_{trans}}{k_t} - \frac{N_i D_i}{k_c} - \gamma_N N_i \tag{1}$$

$$\frac{dD_i}{dt} = \beta_D \frac{1}{1+R^m} - \frac{N_i D_{trans}}{k_t} - \frac{N_i D_i}{k_c} - \gamma_D D_i \tag{2}$$

$$\frac{dR_i}{dt} = \beta_R \frac{(N_i D_{trans})^s}{k_{RS} + (N_i D_{trans})^s} - \gamma_R R_i \tag{3}$$

The parameters β_N, β_D, β_R and γ_N, γ_D, γ_R are the production and degradation rates of Notch, Delta and the Reporter of Notch signalling respectively. The constants k_t and k_c determine the strength of Delta-Notch interactions in trans and in cis respectively, and k_{RS} is the dissociation constant for the intracellular signal. D_{trans} and N_{trans} indicate the incoming Delta and Notch signal and are determined by summing the signal from all contacting cells, scaled by a factor α_a and α_b for apical and basal contacts respectively. We normalized these values so that α_a =1 and α_b =0.2. These relative weighs for apical and basal signalling are in agreement with previously measured values, although our model is relatively robust to changes in α_b (S2). A Gaussian noise term was applied to initiate protein consecrations and to the concentrations at each time step.

Protrusion dynamics

Basal protrusions were implemented as 2D circular areas, extending from the centre of each cell. Radii were drawn from a normal distribution with mean Fmean = 5.6 (2.3 times the cell diameter) and variance 0.3 (S2). A contact probability term was introduced to account for the angular directions of protrusions that were observed and hence the associated likelihood of two protrusions signalling to each other at different ranges. This was implemented in the model by assigning each cell a randomly selected 'direction' term, r, an integer between 1 and 100. For any two cells (cell_1 and cell_2) spaced a distance, d, such that their protrusions are of sufficient length to signal, a signal occurs if the condition is met such that: $vertr_{Cell_1} - r_{Cell_2}| < \frac{P}{d^2}$, where P was a constant variable. Hence the likelihood of a contact being made

reduced in proportion to the square of the distance between two cells. At each time step a random number generator was used to determine whether the protrusions of a particular cell (i.e. the length and directionality of the protrusion) would be updated. Thus, protrusion lifetimes were set according to a Poison distribution.

Cell division

We model cell division in wild-type flies by assuming that cdc25 activity is coupled to the expression of the intracellular Notch reporter, R. The cumulative expression of R at division scales linearly with the division time in control experiments, whereas the value of R itself appears to fluctuate within a confined window (Fig. 3). These data suggest that cells respond to the absolute, rather than cumulative, signal expression, and divide with a probability that is a function of their intracellular Notch expression. To model cell division in this manner, we define,

$$p_d = \frac{R^q}{K_R^q + R^q} \tag{4}$$

where p_d is the probability that a cell divides within a each time step in our simulations, K_R is the hill function dissociation constant and determined the range of values of R for which division is likely. We note that a similar set-up where cdc25 was coupled to the cumulative expression of the Notch reporter gave similar results (not shown). Cells that have divided maintain their expression levels prior to division but no longer participate in lateral signalling so that they are excluded from the calculation of N_{trans} and D_{trans} for other cells. Also note that we set a threshold in the simulation time t_{th} below which cells cannot enter division. This is important in the model because the early dynamics of Delta-Notch are so that most cells go through transient phases where they express both proteins and we want to avoid division at that stage (S3).

Simulation Parameters

The same baseline parameters used for all simulations: $\beta_N = 100$, $\beta_D = 500$, $\beta_R = 300000$, $\gamma_N = \gamma_D = \gamma_R = 1$,$k_t = k_c = 1$, $k_{RS} = 10000000$, $m = 2$, $s = 2$, $q = 5$, Fmean = 5.6, Fse = 0.3, Frate = 10, error = 0.01, $\alpha_a = 1$, $\alpha_b = 0.2$, P=1000 and t_{th}=2. Initial expression values were sampled from a Normal distribution N($10^{-3}\beta_N$, $10^{-4}\beta_N$) and N($10^{-3}\beta_D$, $10^{-4}\beta_D$) for Notch and Delta respectively. All R values were initially set to 0. The cell radius was set equal to 2. We varied the division rule (e.g. dependence on

Delta or intracellular Notch expression), in individual simulations as summarized in each figure legend.

The model was applied to a uniform hexagonally packed 2D array of 50x50 cells. Simulations were performed by numerically solving equations (1)-(3) using the Euler method. The Euler step was set to 0.005 and all simulations were run until stability was reached (defined as no changes in cell fate for 2a.u. of time), which was within T=40a.u. in simulation time.

Supplemental References

[S1]. Sprinzak D, Lakhanpal A, LeBon L, Garcia-Ojalvo J, Elowitz MB. Mutual Inactivation of Notch Receptors and Ligands Facilitates Developmental Patterning. PLoS Comput Biol. 2011 7(6):e1002069.

[S2]. Cohen M, Georgiou M, Stevenson NL, Miodownik M, Baum B. Dynamic filopodia transmit intermittent Delta-Notch signaling to drive pattern refinement during lateral inhibition. Dev Cell. 2010 Jul 20 19(1):78-89.

[S3]. Collier JR, Monk N a, Maini PK, Lewis JH. Pattern formation by lateral inhibition with feedback: a mathematical model of delta-Notch intercellular signalling. J Theor Biol. 1996 183(4):429-46.